

Measurement of the Restoring Forces Acting on Two Optically Bound Particles from Normal Mode Correlations

N. K. Metzger,^{1,*} R. F. Marchington,¹ M. Mazilu,¹ R. L. Smith,² K. Dholakia,^{1,3} and E. M. Wright^{3,1}

¹*SUPA, School of Physics and Astronomy, University of St. Andrews, North Haugh, St. Andrews, KY16 9SS, United Kingdom*

²*Department of Physics, Illinois Wesleyan University, Bloomington, Illinois 61701, USA*

³*College of Optical Sciences and Department of Physics, University of Arizona, Tucson, Arizona 85721, USA*

(Received 7 August 2006; published 7 February 2007)

Optical binding along the axis of two counterpropagating laser fields may be used to organize microparticles into longitudinal, spatially separated, arrays. Here we investigate correlations between the displacements of two optically bound microparticles from their equilibrium positions due to noise. Measurement of the decay time of the correlation functions of the center of mass and relative normal modes is shown to provide an *in situ* method to determine the optical restoring forces acting on the bound particles, thereby providing a test of our physical understanding of longitudinal optical binding.

DOI: [10.1103/PhysRevLett.98.068102](https://doi.org/10.1103/PhysRevLett.98.068102)

PACS numbers: 87.80.Cc

Introduction.—Colloidal suspensions are now established as powerful and controllable systems that may give insights into a wide range of physical systems. A monodisperse colloidal solution has a well-defined thermodynamic temperature and offers a method by which to test theories in strongly interacting physical systems such as liquids as well as insights into aspects of condensed matter physics [1,2]. Colloids may be influenced by the application of an external energy potential landscape which opens up a whole host of studies and may offer an exciting prospect of large scale particle organization. Within this remit the use of optical forces has proven to be very powerful, creating energy landscapes where typically each colloidal particle may find a position, due to the optical gradient force, that minimizes its free energy in such an optical landscape [3–5]. Colloidal interactions are typically complex because they are solvent mediated. Multiple trap sites and energy landscapes can measure hydrodynamic interactions between increasingly large collections of particles—these many-body, long-range interactions control the flow properties of suspensions [6–8]. The pair potential between two particles, $U(r)$, which controls thermodynamic behavior (such as the crystallization which is central to photonic applications), is also inherently many bodied such that $U(r)$ depends on the positions of all particles.

In contrast to predefined optical landscapes the very light-matter interaction between a colloidal particle and an applied optical field can produce significant light redistribution which in turn can affect the optical forces acting on adjacent particles. This underlies the phenomena of optical binding which has recently seen major interest [9–12], whereby self-organized arrays of particles create and mediate their trapping positions via interaction with applied laser fields. A key example of this phenomenon is longitudinal optical binding in a counterpropagating beam geometry whereby microparticles become self-organized

into longitudinal arrays, and which has shown interesting nonlinear and bistable behavior [11,13].

Although considerable progress has been made, the physics underlying optical binding is still not fully understood. In this Letter we experimentally and theoretically explore the optical forces acting on a pair of optically bound particles. The measured forces are found to be in good agreement with numerical calculations for particles in the Mie size regime, thereby providing a test of our physical understanding of longitudinal optical binding. In particular, we present the first data and analysis on the correlated behavior of an array of two optically bound microparticles in the presence of noise, and show that measurement of the decay time of the correlation functions of the center of mass and relative normal modes provides an *in situ* method for determining the optical restoring forces. We note that hydrodynamic coupling between two individually trapped (but not optically coupled) spheres has been observed showing time-delayed anticorrelation [6–8]; however, to date no such studies have been performed in optically bound systems where the optical coupling plays a prominent role.

Theoretical model.—To model the correlated motion between two optically bound spheres we employ the theoretical approach of Meiners and Quake [7] and Bartlett *et al.* [8], which includes the hydrodynamic coupling between the spheres, and we extend the theory to include the optical coupling between the particles. The two identical spheres are assumed optically bound along the z axis by a pair of mutually incoherent but otherwise identical counterpropagating laser fields in a dual beam fiber trap. The spheres of radius “ a ” are taken to have an equilibrium separation R , and we label the deviations of the sphere centers from their equilibrium positions along the z axis by $z_j(t)$, $j = 1, 2$. We assume that the spheres are tightly bound in the plane transverse to the laser propagation axis due to the confinement provided by the Gaussian

intensity profiles, and hereafter concentrate on the longitudinal motions along the z axis. Then adopting the notation of Bartlett *et al.* [8] the Langevin equations of motion for small amplitude sphere displacements can be written in matrix form as

$$\frac{d}{dt} \begin{pmatrix} z_1 \\ z_2 \end{pmatrix} = \begin{pmatrix} A_{11} & A_{12} \\ A_{12} & A_{11} \end{pmatrix} \begin{pmatrix} f_1(t) - kz_1 + \xi z_2 \\ f_2(t) - kz_2 + \xi z_1 \end{pmatrix}. \quad (1)$$

Here $A_{11} = 1/(6\pi\eta a)$ and $A_{12} = 1/(4\pi\eta R)$ detail the longitudinal mobilities, η being the viscosity, $f_j(t)$ are randomly fluctuating functions with correlation functions $\langle f_j(t) \rangle = 0$ and $\langle f_i(t)f_j(t') \rangle = 2(A^{-1})_{ij}k_B T \delta(t - t')$, representing the fluctuating forces acting on the spheres with effective temperature T to account for Brownian and other noise sources, e.g., beam pointing fluctuations, the force terms proportional to the spring constant $k \geq 0$ represent the direct force on a chosen sphere when that sphere is displaced while the other sphere is held fixed, and the force terms proportional to ξ describe the cross force that arises on the chosen sphere at its equilibrium position when the other sphere is displaced. Compared to previous studies by Meiners and Quake [7] and Bartlett *et al.* [8] the new ingredient considered here is the cross force term. The cross force coefficient ξ is positive by virtue of the following physical argument: Longitudinal optical binding arises from the fact that the force acting on a given sphere, say sphere 1, is composed of two components along the z axis, a direct force directed along the positive z axis from the laser field emanating from fiber 1 which is closest to sphere 1, and a second oppositely directed cross force arising from the counterpropagating laser field emanating from fiber 2, and that is refocused onto sphere 1 by sphere 2 (see Fig. 1). Balancing of these two forces results in the equilibrium separation for the two optically bound spheres. If sphere 2 is displaced from its equilibrium position and slightly away from sphere 1, then the focus produced by sphere 2 on the field from fiber 2 will likewise be moved away from sphere 1. This implies that the cross force acting on sphere 1 will be reduced in comparison to the direct force, so that sphere 1 will move in the direction of the displacement of sphere 2, which implies $\xi \geq 0$. The cross force thus tends to correlate the motions of the two spheres.

To proceed we introduce the normal mode coordinate $Z_1 = (z_1 + z_2)/2$ for the center of mass motion, and the normal mode coordinate $Z_2 = (z_1 - z_2)$ for the relative motion [7,8]. Then applying the same theoretical approach described by Bartlett *et al.* [8] to the above model we find the correlation functions ($j = 1, 2$)

$$C_j(t) = \frac{\langle Z_j(t)Z_j(0) \rangle}{\langle Z_j^2(t) \rangle} = \exp(-|t|/\tau_j), \quad (2)$$

where t is the delay time, and the decay times for the center of mass ($j = 1$) and relative ($j = 2$) normal modes are given by

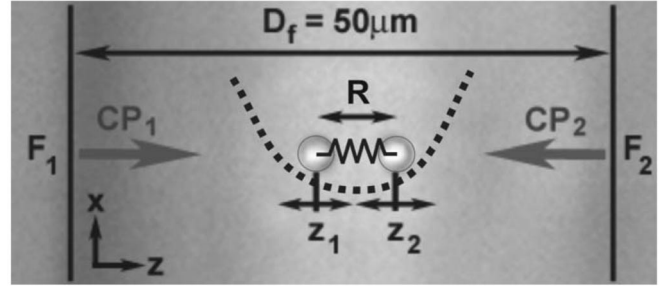


FIG. 1. Fiber optical trap setup: the counterpropagating light fields (CP_1 and CP_2) at 1070 nm emerge from two single mode fibers (F_1 and F_2) with a separation of the fiber facets D_f . The array is formed in the gap between the two fibers with R being the equilibrium separation of the spheres centers and $z_{1,2}$ indicate small displacements from the equilibrium position of the two spheres along the z axis. The array center of symmetry ($R/2$) coincides with half the fiber separation ($D_f/2$). The two normal modes of the bound array are highlighted in the graphic: The dashed line represents the potential related to the center of mass motion of the two-sphere system. The spring between the two spheres indicates the optical cross interaction between the spheres, the relative motion of them within the system.

$$\begin{aligned} \frac{1}{\tau_1} &= kA_{11}(1 + \varepsilon)[1 - (\xi/k)], \\ \frac{1}{\tau_2} &= kA_{11}(1 - \varepsilon)[1 + (\xi/k)]. \end{aligned} \quad (3)$$

Here $\varepsilon = A_{12}/A_{11} = 3a/(2R)$, and since the sphere spacing R will be somewhat larger than the sphere radius a we have $\varepsilon < 1$. Furthermore, stability of the optically bound state requires that the correlation decay times be positive, which yields the condition $(\xi/k) < 1$ for stability.

Experimental measurement of the correlation decay times can yield the restoring forces of the optical binding of the two particles around the equilibrium. By dividing the two decay times and rearranging we obtain

$$\left(\frac{\xi}{k}\right) = \left[\frac{(1 + \varepsilon)/(1 - \varepsilon) - \tau_2/\tau_1}{(1 + \varepsilon)/(1 - \varepsilon) + \tau_2/\tau_1} \right]. \quad (4)$$

Since $\varepsilon = 3a/(2R)$ is a known parameter, by measuring the normal mode decay times $\tau_{1,2}$ we have an *in situ* method of measuring the ratio (ξ/k) of the cross and direct force coefficients, and the direct force coefficient k may then be found using Eq. (3). The direct force constant clearly plays the role of a trap stiffness and could be measured using standard methods for single particle traps, see, for example, Ref. [14]. The new element here is the cross force term which is an inherently multiparticle effect (illustrated in Fig. 1 as a spring between the spheres), and hence our proposal for a new approach based on particle correlations is required.

The direct and cross force coefficients can also be calculated theoretically for particles in the Mie size regime using the wave optics approach described in Ref. [13]. As

an example to be compared against the experiment consider the case of two counterpropagating Gaussian laser beams of wavelength $1.07 \mu\text{m}$, spot size $w_0 = 3.4 \mu\text{m}$, and waist (fiber) separation $50 \mu\text{m}$, and two particles of radius $= 1.5 \mu\text{m}$ and refractive-index $n_s = 1.41$ imbedded in a host liquid of refractive index $n_h = 1.328$ (deuterium). The small index difference $(n_s - n_h) = 0.082$ between the sphere and host medium combined with the fact that the sphere is in the Mie size regime means that the paraxial wave theory of Ref. [13] is applicable. Then we find an equilibrium spacing $R = 6.9 \mu\text{m}$, giving $\varepsilon = 0.326$, and $k = 0.31 \text{ pN}/\mu\text{m}$, $\xi = 0.24 \text{ pN}/\mu\text{m}$, and $(\xi/k) = 0.78$ for a laser power of 110 mW [The raw numerical data for the direct (crosses) and cross (circles) forces are shown in Fig. 2(a)]. Both the direct and cross force coefficients scale linearly with the laser input power so that the ratio (ξ/k) is independent of laser power.

Experiment.—A dual beam fiber optical trap [15] as illustrated in Fig. 1 was used for our experimental studies, and is discussed in detail elsewhere [11,13,16]. The two opposing fibers (marked F_1 and F_2 in Fig. 1) were operated using light from a continuous wave ytterbium fiber laser (IPG Photonics) at $\lambda = 1070 \text{ nm}$ with an optical isolator to avoid perturbations of the laser due to back reflections. The laser coherence length was very short and the experimental beam path ensured we could ignore any interference effects. The light was coupled into a single mode fiber of mode size $3.4 \mu\text{m}@1070 \text{ nm}$. It is split into two equal beams via a 2×2 fiber splitter (OZ optics) with a 50:50 splitting ratio to provide equal field power distributions within the trap of 110 mW from each fiber. Additionally the back coupled light from fiber F_1 into F_2 and vice versa was measured with a power meter at the fiber splitter's second in-coupling port (similar to a Sagnac fiber interferometer setup) to observe and eradicate long term drift of

the coupling setup. This enables us to achieve overall light intensity stability within the trap of better than 7% over multiple experimental realizations. To further ensure symmetric array formation at half the fiber separation one arm could also be attenuated by a variable fiber attenuator, and the fibers were of different length to avoid standing wave effects. The sample chamber consisted of a polydimethylsiloxane (PDMS) microfluidic structure in which the two fibers were embedded to form a counterpropagating fiber trap with a fixed separation D_f between the fiber surfaces. The setup was allowed to temperature stabilize to $20 \text{ }^\circ\text{C} \pm 0.5 \text{ }^\circ\text{C}$.

A monodisperse mixture of $3 \mu\text{m}$ silica microspheres in deuterium dioxide (D_2O) was injected through a $100 \mu\text{m}$ flow channel, perpendicular to the fiber trap. The microfluidic structure was hermetically sealed to prevent evaporation and flow within the sample. A helper tweezer allowed the initialization (loading) of the array and allowed a low sphere density within the sample. The two-sphere array was observed via a microscope objective (Nikon plan oil-immersion 50×0.9) onto the CCD array of a fast camera (Basler A622f) with a data acquisition rate of $\Delta t = 0.0026 \text{ s}$; Fig. 1 contains a typical frame of the captured video as an underlaid background image. Following the approach of [6], the captured frames were analyzed utilizing an IDL based particle tracking software [17] and the particle position in $z_{1,2}$ extracted with an accuracy of better than 50 nm to sufficiently capture the rms displacement of the individual spheres of about 120 nm . Subsequent data processing involved compensation of an angular offset of the z axis to avoid crosstalk between the z and x coordinates of the spheres. Over a period of 26 sec the center of mass coordinate $Z_1 = (z_1 + z_2)/2$ for the two particles, and the relative coordinate $Z_2 = (z_1 - z_2)$ was determined, as the correlation timescale of the sphere system is expected to be at the order of seconds. From 25 of these data

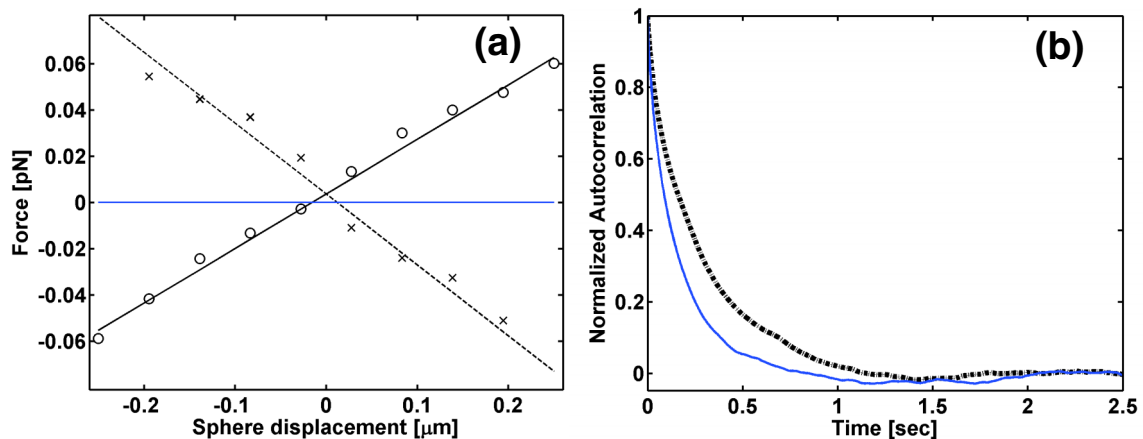


FIG. 2 (color online). (a) Theoretical calculation of the direct (crosses) and cross (circles) force components, from the slope of the linear fit the coefficients for ξ/k can be deduced to $k = 0.31 \text{ pN}/\mu\text{m}$ and $\xi = 0.24 \text{ pN}/\mu\text{m}$, respectively. (b) Normalized autocorrelation functions averaged over 25 consecutive data sets for the center of mass normal mode (dashed line) yielding $\tau_1 = 0.26 \text{ s}$, and relative normal mode (solid line) giving $\tau_2 = 0.14 \text{ s}$.

sets the averaged autocorrelation functions was calculated to determine the correlation decay times τ_1 and τ_2 .

Results.—The following experiments were carried out using an array of two $3\ \mu\text{m}$ diameter spheres, a fiber separation $D_f = 50 \pm 2\ \text{mm}$, and an output power of 110 mW emerging from each fiber. The experimentally observed value of the averaged center to center separation (R) of the array of $6.7\ \mu\text{m}$ is in acceptable agreement with the theoretical value of $6.9\ \mu\text{m}$. The experimentally measured correlation functions are shown in Fig. 2(b), and show the expected decay with increasing delay time. The nonexponential decay evident for delays larger than 0.5 sec may be due to sampling issues related to the finite size of the data sets and are similar to that reported in Ref. [6]. By varying the data set size we have ensured that results for delays less than 0.5 sec are robust against variations.

By reading the normal mode decay times $\tau_{1,2}$ from the data as the delay times at which the autocorrelations drop to $1/e$, which occurs for delays less than 0.5 sec, we obtain $\tau_1 = 0.26\ \text{sec}$ and $\tau_2 = 0.14\ \text{sec}$. Using Eq. (4) we then find the experimentally determined ratio of the cross and direct force coefficients $(\xi/k) = 0.72$, in contrast to the theoretical value of $(\xi/k) = 0.77$, and using Eqs. (3) and (4) we find $k = 0.29\ \text{pN}/\mu\text{m}$ experimentally, in comparison to the theoretical value of $k = 0.31\ \text{pN}/\mu\text{m}$. Thus, we have acceptable agreement between the theory and experiment for the optical forces acting on the two microparticles in the optically bound array.

Conclusion.—In conclusion, we have demonstrated the utility of measuring particle correlations as a means of measuring the optical forces acting within optically bound arrays. We also observe excellent agreement between the measured optical forces and numerical simulations for particles in the Mie size regime, thereby providing a key test of our physical understanding of longitudinal optical binding. Measuring the optical force coefficients means that the full linear response of the optically bound system around its equilibrium, encapsulated in Eq. (1), is now attained so that one may now explore the response of the system to external modulations using, e.g., external tweezers. Our results are also an important step towards exploring the nonlinear response of optically bound arrays for large amplitude modulations.

We thank Dr. Erik Baigar, Dr. Robert R. J. Maier, and Professor Gabriel Spalding for fruitful discussions. This work was supported by the European Commission Sixth Framework Programme—NEST ADVENTURE Activity—, through Project ATOM-3D (No. 508952) and the European Science Foundation EUROCORES Programme SONS (Project NOMSAN) by funds from the UK Engineering and Physical Sciences Research Council and the EC Sixth Framework Programme. R. L. S. was supported by the Petroleum Research Fund. E. M. W. is funded in part by the Joint Services Optical Program (JSOP).

*Corresponding author.

Electronic address: nkm2@st-and.ac.uk

- [1] A. Chowdhury, B. J. Ackerson, and N. A. Clark, Phys. Rev. Lett. **55**, 833 (1985).
- [2] C. Bechinger, M. Brunner, and P. Leiderer, Phys. Rev. Lett. **86**, 930 (2001).
- [3] M. P. MacDonald *et al.*, Science **296**, 1101 (2002).
- [4] H. Melville *et al.*, Opt. Express **11**, 3562 (2003).
- [5] Y. Roichman and D. G. Grier, Opt. Express **13**, 5434 (2005).
- [6] M. Polin, D. G. Grier, and S. Quake, Phys. Rev. Lett. **96**, 088101 (2006).
- [7] J. C. Meiners and S. R. Quake, Phys. Rev. Lett. **82**, 2211 (1999).
- [8] P. Bartlett, S. I. Henderson, and S. J. Mitchell, Phil. Trans. R. Soc. A **359**, 883 (2001).
- [9] M. M. Burns, J.-M. Fournier, and J. A. Golovchenko, Science **249**, 749 (1990).
- [10] S. A. Tatarkova, A. E. Carruthers, and K. Dholakia, Phys. Rev. Lett. **89**, 283901 (2002).
- [11] W. Singer *et al.*, J. Opt. Soc. Am. B **20**, 1568 (2003).
- [12] M. Guillon, O. Moine, and B. Stout, Phys. Rev. Lett. **96**, 143902 (2006).
- [13] N. K. Metzger, K. Dholakia, and E. M. Wright, Phys. Rev. Lett. **96**, 068102 (2006).
- [14] K. C. Neuman and S. M. Block, Rev. Sci. Instrum. **75**, 2787 (2004).
- [15] A. Constable *et al.*, Opt. Lett. **18**, 1867 (1993).
- [16] N. K. Metzger *et al.*, Opt. Express **14**, 3677 (2006).
- [17] J. C. Crocker and D. G. Grier, J. Colloid Interface Sci. **179**, 298 (1996).